Heat Mass Transfer (2011) 47:1089–1099
DOI 10.1007/s00231-011-0773-0

ORIGINAL

Investigation of the different base fluid effects on the nanofluids heat transfer and pressure drop

Javad Bayat · Amir Hossein Nikseresht

Received: 11 July 2010 / Accepted: 16 February 2011 / Published online: 5 March 2011

Abstract A numerical study of laminar forced convective flows of three different nanofluids through a horizontal circular tube with a constant heat flux condition has been performed. The effect of Al_2O_3 volume concentration $0 \leq \varphi \leq 0.09$ in the pure water, water-ethylene glycol mixture and pure ethylene glycol as base fluids, and Reynolds number of $100 \leq \mathrm{Re} \leq 2{,}000$ for different power inputs in the range of $10 \leq Q(W) \leq 400$ have been investigated. In this study, all of the nanofluid properties are temperature and nanoparticle volume concentration dependent. The governing equations have been solved using finite volume approach with the SIMPLER algorithm. The results indicate an increase in the averaged heat transfer coefficient with increasing the mass of ethylene glycol in the water base fluid, solid concentration and Reynolds number. From the investigations it can be inferred that, the pressure drop and pumping power in the nanofluids at low solid volumetric concentration ($\varphi < 3\%$) is approximately the same as in the pure base fluid in the various Reynolds numbers, but the higher solid nanoparticle volume concentration causes a penalty drop in the pressure. Moreover, this study shows it is possible to achieve a higher heat transfer rate with lower wall shear stress with the use of proper nanofluids.

List of symbols

C_p	Specific heat, (J/kg K)
D	Diameter of tube, (m)
g	Gravitational acceleration, (m/s^2)
$h(x)$	Heat transfer coefficient, $q''/(T_w(x) - T_b(x))$ (W/m^2 K)
h_m	Averaged Heat transfer coefficient, $\frac{1}{L}\int_0^L h(x)dx$
k	Thermal conductivity, (W/m K)
L	Length of the tube, (m)
$Nu(x)$	Local Nusselt number, $h(x)$ D/K
$\overline{Nu}$, Nu_m	Averaged Nusselt number, h_m D/K
P	Pressure, (N/m^2)
Pe_d	Particle Peclet number, $u_m d_p/\alpha_{nf}$
Pr	Prandtl number, $\mu\ C_p/k$
q''	Uniform heat flux, (W/m^2)
Q	Heat transfer rate, (W)
r	Radial coordinate and radius, (m)
Re	Reynolds number, $\rho\ U_0 D/\mu$
T	Temperature, (K)
u,U	Component of velocity, (m/s)
x	Distance from the inlet, (m)

Greek symbols

α	Thermal diffusivity, $k/(\rho C_p)$ (m^2/s)
φ	Volume fraction
μ	Dynamic viscosity, (N/s m^2)
ν	Kinetic viscosity, (m^2/s)
ρ	Density, (kg/m^3)
τ (S)	Wall shear stress, (N/m^2)

Subscripts

bf	Base fluid
d	The contribution of hydrodynamic dispersion and irregular movement of the nanoparticles
eff	Effective
m	Average
nf	Nanofluid
p	Nanoparticle

J. Bayat · A. H. Nikseresht (✉)
Mechanical Engineering Department,
Shiraz University of Technology, Shiraz, Iran
e-mail: nikser@sutech.ac.ir

J. Bayat
e-mail: javad.Bayat@gmail.com

w Wall
0 Inlet condition

1 Introduction

The improvement of convective heat transfer in various industrial processes is required. There are several ways to enhance the convective heat transfer, including increasing the area, altering the boundary conditions, changing the flow regime, using roughen surface or groove and rib. But the traditional heat transfer fluid such as water, oil, or ethylene glycol which have poor heat transfer characteristics prevent increasing energy efficiencies. One way to improve heat transfer rate is to increase thermal conductivity of the fluid. A nanofluid is a suspension of solid nanoparticles (normally less than 100 nm diameters) in conventional liquids. With respect to the thermal properties of the solid nanoparticles the liquid thermal conductivity can be increased. Indeed, most solids, especially metals have thermal conductivities much higher than fluids. Hence, the fluid containing solid particles may significantly increase its conductivity [1–6]. After the newly born nanofluid method with suspended nanometer sized particles was proposed by Cho [1]; many researchers have investigated the characteristics of nanofluids. Sohn and Chen [7] reported that by adding small solid particles in liquid, the heat transfer coefficient can considerably be augmented. Wen and Ding [8] have studied Al_2O_3/water nanofluid heat transfer in laminar flow under wall heat flux and reported an increase in nanofluid heat transfer coefficient with increasing Reynolds number and nanoparticles concentration. The reason for heat transfer enhancement in nanofluids is the decrease of thermal boundary layer thickness due to random movement of particles which takes a major role in increasing the heat transfer rate between the fluid and the wall. Xuan et al. [9] have examined the transport properties of nanofluids, and a review of convective heat transfer using nanofluids has been presented by Wang and Mujumdar [10] which summarizes research work on heat transfer characteristics. Li and Xuan [5] reported the empirical correlation for computing the Nusselt number in both laminar and turbulent tube flow using water with TiO_2 and Al_2O_3 particles. They have shown a remarkable increase of the heat transfer capability of the base fluid. In the laminar fully developed flow they proposed:

$$Nu_{nf} = \frac{h_{nf}D}{k_{nf}} = 0.4328\ (1.0 + 11.285\varphi^{0.754}pe_d^{0.218})\mathrm{Re}_{nf}^{0.333}pr_{nf}^{0.4} \quad (1)$$

Roy et al. [11] investigated numerical study of laminar flow heat transfer Al_2O_3-EG and Al_2O_3-water and reported an improvement in the heat transfer rate. Also they showed that wall shear stress increases with increasing nanoparticles concentration and Reynolds number. Maiga et al. [12], have numerically investigated the hydrodynamic and thermal behavior of Al_2O_3-water and Al_2O_3-EG nanofluid flowing inside a uniformly heated tube. For laminar flow a considerable increase in heat transfer has been observed with an increase on solid volume fraction with respect to the base flow. Also it has been found that the augmentation of nanoparticles illustrated drastic adverse effects on the wall shear stress. A correlation for computing the averaged Nusselt number under constant heat flux has been proposed by them:

$$Nu_m = 0.086\mathrm{Re}_{nf}^{0.55}pr_{nf}^{0.5} \quad \text{for} \quad 6 \le pr \le 753; \quad \mathrm{Re} \le 1000; \quad \varphi \le 10\% \quad (2)$$

In this study, the laminar convective flows of three stable nanofluids EG, water, and EG/water mixture 60:40 by mass and Al_2O_3 as nanoparticle in an axi-symmetric horizontal tube with constant heat flux for varying heat transfer rate, Reynolds number and nanoparticle concentration are studied. The aim of this research is to investigate the comparison of different base fluid nanofluid to achieve higher heat transfer with less wall shear stress.

2 Governing equations and mathematical modeling

Figure 1 shows the schematic representation of the system used in this study. The flow is an axi-symmetric steady, forced laminar convection flow of nanofluid through a horizontal circular tube, having diameter $D = 4.57$ mm and a length of $L = 2$ m. The length of the tube is very large compared to its diameter. It is assumed that the base fluid and solid particles are in thermal equilibrium with zero relative velocity which is demonstrated through the experimental results [9, 13, 14], so single phase fluid procedure with variation of all effective thermo physical properties can be applied. Table 1 presents thermo physical properties of base fluids and nanofluids which corporate in the present analysis.

The governing equations for axi-symmetric coordinates are as follows [15]:

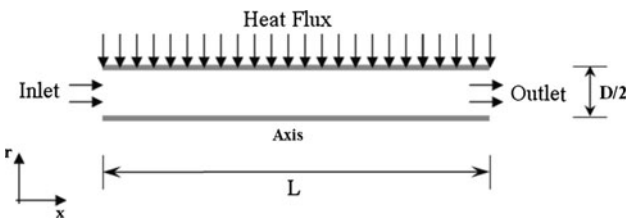

Fig. 1 Geometrical configuration of the present problem

Table 1 Thermophysical properties of the nanofluids at the inlet temperature

Type of fluid	Nanoparticles concentration (φ)	Thermal conductivity [W m^{-1} k^{-1}]	Viscosity [mN s m^{-2}]	Specific heat [J kg^{-1} k^{-1}]	Density [kg m^{-3}]
Water	0.00	0.606	0.96	4,183.32	997.51
Water/Al_2O_3	1.50	0.629	1.09	3,987.5	1,042.10
Water/Al_2O_3	3.00	0.656	1.27	3,808.43	1,086.69
Water/Al_2O_3	5.00	0.693	1.60	3,590.64	1,146.14
Water/Al_2O_3	7.00	0.733	2.03	3,394.86	1,205.59
Water/Al_2O_3	9.00	0.775	2.54	3,217.55	1,265.04
EG	0.00	0.251	19.36	2,396.58	1,117.64
EG/Al_2O_3	3.00	0.278	24.58	2,235.64	1,203.21
EG-Water	0.00	0.350	5.02	3,092.93	1,084.99
EG-Water/Al_2O_3	3.00	0.382	6.49	2,864.68	1,171.54
EG-Water/Al_2O_3	5.00	0.404	7.75	2,712.54	1,229.24
EG-Water/Al_2O_3	9.00	0.451	14.02	2,348.86	1,423.41

Continuity:

$$\frac{1}{r}\frac{\partial}{\partial x}(\rho_{nf}V_x)+\frac{\partial}{\partial x}(\rho_{nf}V_r)+\frac{\rho_{nf}V_r}{r}=0 \tag{3}$$

Momentum:

$$V_r\frac{\partial V_x}{\partial r}+V_r\frac{\partial V_x}{\partial x}=-\frac{1}{\rho_{nf}}\frac{\partial p}{\partial x}+\nu_{nf}\left(\frac{1}{r}\frac{\partial}{\partial r}\left(r\frac{\partial V_x}{\partial r}\right)+\frac{\partial^2 V_x}{\partial x^2}\right) \tag{4}$$

$$V_r\frac{\partial V_r}{\partial r}+V_r\frac{\partial V_r}{\partial x}=-\frac{1}{\rho_{nf}}\frac{\partial p}{\partial r}+\nu_{nf}\left(\frac{1}{r}\frac{\partial}{\partial r}\left(r\frac{\partial V_r}{\partial r}\right)+\frac{\partial^2 V_r}{\partial x^2}-\frac{V_r}{r^2}\right)+g_r \tag{5}$$

Energy:

$$V_r\frac{\partial T}{\partial r}+V_r\frac{\partial T}{\partial x}=\alpha_{nf}\left(\frac{1}{r}\frac{\partial}{\partial r}\left(r\frac{\partial T}{\partial r}\right)+\frac{\partial^2 T}{\partial x^2}\right) \quad \text{where } \alpha_{nf}=\frac{k_{nf}}{(\rho C_p)_{nf}}. \tag{6}$$

The physical and thermal properties such as density, viscosity, specific heat, and thermal conductivity of the nanofluids are calculated using different appropriate formulae which are as follows:

The density of the nanofluids is calculated according to Pak and Cho's equation [13]:

$$\rho_{nf}=\varphi\ \rho_p+(1-\varphi)\rho_{bf} \tag{7}$$

where φ and ρ_p are the volume fraction and density of the nanoparticles and ρ_{bf} is the density of the base fluid. The followings are two different formulas for calculating the specific heat of nanofluids.Pak and Cho's equation [13]:

$$c_{nf}=\varphi\ c_p+(1-\varphi)c_{bf} \tag{8}$$

Xuan and Roetzel's equation [16]:

$$c_{nf}=\frac{\varphi\rho_p\ c_p+(1-\varphi)\rho_{bf}c_{bf}}{\rho_{nf}} \tag{9}$$

The volume-averaged (8) yields poor prediction on measured specific heats. In contrast, mass averaged expression which is reported in (9) matches the experimentally-measured values of the specific heat exceptionally well, and is recommended specifically for the nanofluids of interest here [17, 18].

The thermal conductivity of the nanofluids flow can be calculated from the following equations [19]:

For water-Al_2O_3

$$\frac{k_{nf}}{k_{bf}}=4.79\varphi^2+2.72\varphi+1 \tag{10}$$

For ethylene glycol-Al_2O_3

$$\frac{k_{nf}}{k_{bf}}=28.905\varphi^2+2.8273\varphi+1 \tag{11}$$

For evaluating the thermal conductivity of EG/water-Al_2O_3 nanofluid Vajjha and Das [20], proposed the following model:

$$k_{nf}=\frac{k_p+2k_{bf}-2\varphi(k_{bf}-k_p)}{k_p+2k_{bf}+\varphi(k_{bf}-k_p)}k_{bf}+5\times 10^4\beta\ \varphi\ \rho_{bf}C_{bf}\sqrt{\frac{\kappa T}{\rho_p\ d_p}}f(T,\varphi) \tag{12}$$

where $f(T,\varphi)$ and β are defined from Vajjha and Das experimental data [20].

$$f(T,\varphi) = (2.8217 \times 10^{-2}\varphi + 3.917 \times 10^{-3})\frac{T}{T_0} + (-3.0669 \times 10^{-2}\varphi - 3.91123 \times 10^{-3})$$

$$\beta = 8.4407\ (100\varphi)^{-1.07304} \quad \text{for } \varphi \leq 10\%$$

The temperature range of the experiments that they used to obtain the above formula is from 298 to 363 K. In the present research the maximum temperature is 298 K which is not in the above range, since in the present work for EG/water-Al_2O_3 nanofluids the thermal conductivity is evaluated as follows [21]:

$$\frac{k_{nf}}{k_{bf}} = \frac{k_p + (n-1)k_{bf} - (n-1)\varphi(k_{bf} - k_p)}{k_p + (n-1)k_{bf} + \varphi(k_{bf} - k_p)} \tag{13}$$

where (n) is defined by $n = 3/\Psi$ and Ψ is ratio of the sphericity defined as the ratio of the surface area of a sphere with volume equal to that of the particle, to the surface area of the particle. Also Zhang et al. [22] have shown that this correlation accurately predicts the thermal conductivity of nanofluids. Moreover in Table 2 a comparison between the Hamilton-Crosser correlation, which is used in the present study, and Vajjha-Das experimental data for EG/water-Al_2O_3 nanofluids at $T = 295$ K [20] is depicted. It is clear that the maximum deviation is 3%.

The viscosity of water-Al_2O_3 nanofluids is calculated from the correlation (14) which is derived by Abu-Nada [23] using the experimental data of Nguyen et al. [24].

$$\mu_{nf} = -0.155 - \frac{19.582}{T} + 0.794\varphi + \frac{2094.47}{T^2} - 0.192\varphi^2 - 8.11\frac{\varphi}{T} - \frac{27463.863}{T^3} + 0.0127\varphi^3 + 1.6044\frac{\varphi^2}{T} + 2.1754\frac{\varphi}{T^2} \quad \text{for } \varphi \leq 9.4\% \tag{14}$$

The above equation is expressed in centi poise. Equation (15) has been obtained for computing the dynamic viscosity of ethylene glycol-Al_2O_3 nanofluid and was reported by Masuda et al. [25].

$$\frac{\mu_{nf}}{\mu_{bf}} = 306\varphi^2 - 0.19\varphi + 1 \tag{15}$$

Viscosity values of EG/water-Al_2O_3 nanofluid were measured by Namburu et al. for 1–10% volume concentration [26]. For EG/water-Al_2O_3 nanofluids the viscosity is evaluated from (16) as follows:

$$Log\ \mu_{nf} = Ae^{-BT} \tag{16}$$

where T is the temperature in Kelvin and ranging from 238 K (−35°C) to 323 K (50°C) and A and B are functions of volumetric concentration (φ).

$$A = -0.29956\varphi^3 + 6.7388\varphi^2 - 55.444\varphi$$
$$B = (-6.4745\varphi^3 + 140.03\varphi^2 - 1478.5\varphi + 20341)/10^6 \tag{17}$$

It should be noted that all of the base fluid properties mentioned in the above equations ρ_{bf},c_{bf},k_{bf}, and μ_{bf} are temperature dependent and curve fitted from ASHRAE data [27]. For example the following correlations for EG/water properties as functions of temperature are used where $273.15 \leq T \leq 373.15$:

$$\rho_{bf} = 1107e^{-\left(\frac{T-203.9}{644.6}\right)^2} + 0.03105e^{-\left(\frac{T-345.8}{23.37}\right)^2} - 61.09e^{-\left(\frac{T-567.7}{82.38}\right)^2} + 0.05255e^{-\left(\frac{T-319.3}{0.7235}\right)^2} + 0.007026e^{-\left(\frac{T-359.8}{2.547}\right)^2} - 0.04174e^{-\left(\frac{T-295.5}{26.58}\right)^2}$$

$$\mu_{bf} = 10410e^{-(0.05138T)} + 0.2019\,e^{-(0.01513T)}$$

$$k_{bf} = 0.3796e^{-\left(\frac{T-381}{198.6}\right)^2} + 0.01284e^{-\left(\frac{T-323.1}{14.21}\right)^2} + 0.006686e^{-\left(\frac{T-309}{9.146}\right)^2} + 0.04143e^{-\left(\frac{T-285.3}{22.89}\right)^2} - 0.002359e^{-\left(\frac{T-343.6}{7.265}\right)^2} + 0.006658e^{-\left(\frac{T-344}{11.16}\right)^2}$$

$$Cp_{bf} = 5471e^{-\left(\frac{T-1107}{1075}\right)^2}$$

The boundary conditions are as follows:

At the tube inlet: $u_x = U_0$; $u_r = 0$; $T = T_0 = 22$°C.

On the wall: $u_x = u_r = 0$ (no-slip condition); $q'' = -k_{nf}\frac{\partial T}{\partial r}$

At the tube outlet: the fully developed conditions prevail.

As mentioned earlier, it is supposed that the continuum assumption is still valid for the fluid with suspended

Table 2 Thermal conductivity of EG-Water/Al_2O_3 nanofluids at the inlet temperature

Type of fluid	Nanoparticles concentration (φ)	Vajjha—Das experimental data [W m^{-1} k^{-1}]	Hamilton—Crosser correlation [W m^{-1} k^{-1}]
EG-Water/Al_2O_3	1.00	0.372243	0.360938
	2.00	0.383485	0.370314
	4.00	0.404418	0.392189
	6.00	0.423777	0.415625
	8.00	0.447843	0.439061

nano-size particles. Thermal equilibrium assumption and no slip boundary conditions, which are validated extensively through the experimental results, have been used. The single phase modeling approach is much easier and more computationally efficient than two-phase modeling approach. So it has more been adopted in the literature and can be feasible for investigation of nanofluids flow. It should be taken into account that the above equations for estimation of the effective viscosity (Eqs. 14 and 16) of Nguyen et al. [24] and Namburn et al. [26] are restricted to 47 nm and 53 nm particle size with the volume fraction in the range of $0 \leq \varphi \leq 9.4\%$ and $1 \leq \varphi \leq 10\%$, respectively.

3 Numerical approaches

The time-independent sets of incompressible coupled nonlinear partial differential equations have been discretized using the finite volume method. A first order upwind scheme has been selected for the convective and diffusion terms while the SIMPLE algorithm has been applied for the velocity–pressure coupling implicitly [28, 29], converged solutions have been considered when the residual in each equation is lower than 10^{-8}. The non-uniform grid has been adopted in the radial and axial directions which is finer at an adjacent tube wall. To obtain a grid independence solution, several different grids have been studied. Figure 2a, and b show the effects of grid densities on the dimensionless velocity at the centerline section of $x/D = 100$, and averaged heat transfer coefficient on the wall. From this grid study it is found that a set of grid system with 200×31 nodes give results with enough accuracy.

4 Results and discussion

In order to illustrate the validity and certitude of the code, at first pure water fluid flow in the tube is solved in a Reynolds number of 1,620. The boundary conditions are chosen similar to [30]. Figure 3 shows the variation of local Nusselt No. versus the dimensionless length (x/D). In this figure the present results have been compared with experimental data of [30], Shah equation [31] and classic theory. The results show good agreement with experimental data. It should be mentioned that the deviation between classic theory values and the present results in the fully developed region, where the classic theory can be applied to, is due to the temperature dependency of thermophysical properties of the base fluid in the present study. It causes higher heat transfer coefficients and Nusselt numbers. Also as can be seen in Fig. 3, the Shah equation

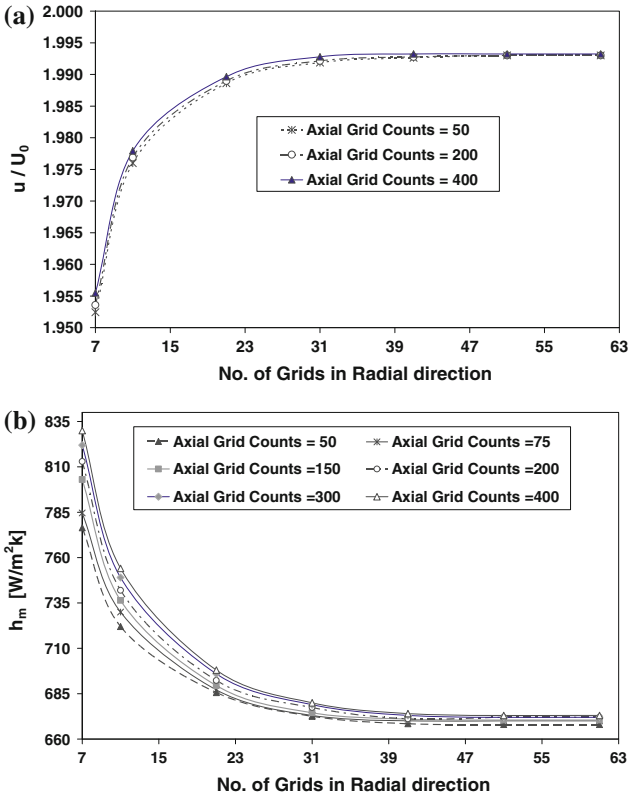

Fig. 2 Grid independency study

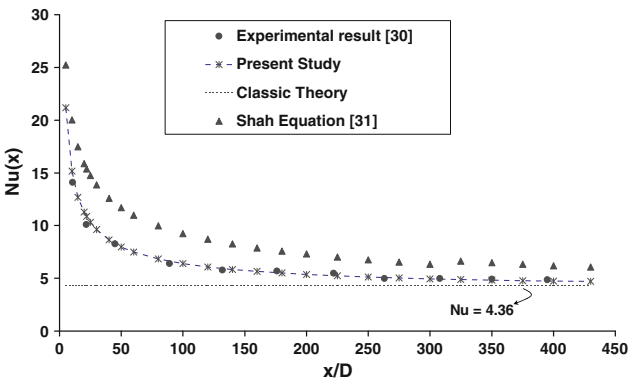

Fig. 3 Comparison of the computed local Nusselt number values with the experimental data and empirical equations for pure water

considerably overestimates the Nusselt number and this is due to the fact that they developed their formulation in large channels, so it can not well predict the results for tubes with small diameter.

Figure 4 shows the local convective heat transfer coefficient of pure water and water-Al_2O_3 3vol% nanofluids at Re = 1,460 in axial position. Also in this figure the present results are compared with experimental data of [30] and an excellent agreement is observed.

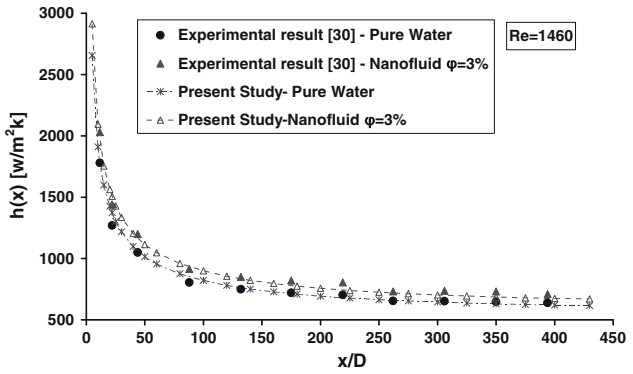

Fig. 4 Comparison of the computed local convective heat transfer coefficient with the experimental data for pure water and alumina nanofluid

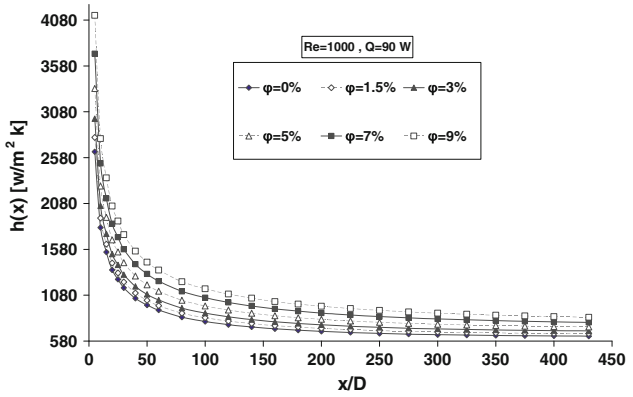

Fig. 5 The effect of solid volume fraction on the heat transfer coefficient of nanofluids for water as a base fluid

In the following, the code was performed to simulate laminar flow with considering three nanofluids, namely pure water, water-ethylene glycol mixture, and pure ethylene glycol with Al_2O_3 nanoparticles volume concentration of $0 \leq \varphi \leq 0.09$, Reynolds No. of $100 \leq Re \leq 2{,}000$, and heat inputs of $10 \leq Q \leq 400$. Results have revealed that the presence of nano-particles has considerable effects on the thermal characteristics of the mixture. Figure 5 displays the heat transfer coefficient of nanofluids with water as the base fluid in a fixed Reynolds number of 1000 and constant heat input of 90 W. An increase in nanoparticles concentration enhances the value of the heat transfer coefficient by about 5.9% to 56% for $\varphi = 1.5\%$ to 9% at the axial position of $x/D = 5$. The enhancement of the heat transfer coefficient decreases with the axial position, for example in the position of the $x/D = 200$ and 400 the increase varies in the range of 4.8% to 40%, and 4.3% to 32% respectively. It should be noted that in the entrance region of the tube the enhancement effect of nanoparticles volume concentration is more prevalent than in the fully

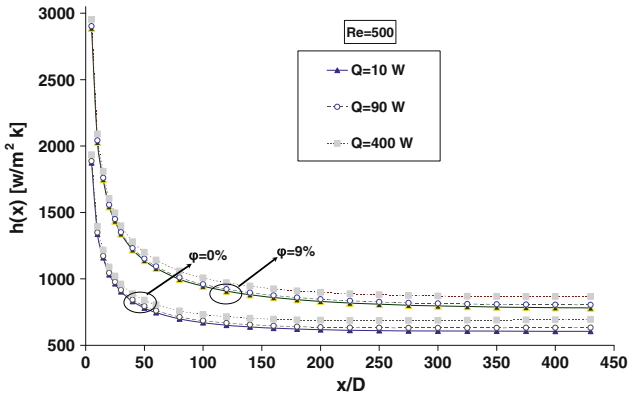

Fig. 6 The effect of different power inputs on the local heat transfer coefficient of nanofluids

developed region. It is presumably because of the influence of the solid particles on the thermal boundary layer.

Many researchers have argued that in fact some factors such as : Brownian interface, thermal conductivity, particle migration, phonon movement, nanoparticle clustering, and reduction of boundary layer thickness are possible mechanisms for heat transfer enhancement in nanofluids [32, 33]. It is difficult to indicate which of these mechanisms are dominant. However, a simple analysis shows that thermal entrance length depends on Prandtl number and it can be concluded that by adding nanoparticles into the base fluid, the entrance region becomes to some extent larger and this affects the enhancement of convective heat transfer.

The effect of heat transfer rate on the local heat transfer coefficient at Re = 500 for two cases of $\varphi = 0\%$ and 9% is presented in Fig. 6. As this figure shows, similar to Fig. 5 the curves gradually decrease along the tube length, moreover increasing Q augments the local heat transfer coefficient. It is interesting to note that, in the fully developed region the enhancement of the heat transfer coefficient by increasing the heat flux is more than of the tube entrance, for instance in the graph of $\varphi = 9\%$ the enhancement of the heat transfer coefficient with increasing heat flux from 10 to 400 W is 2.3% at $x/D = 5$ and is 11% at $x/D = 400$. Figure 7 depicts the influence of nanoparticle volume concentration on the Nusselt number at Re = 1,000 and $Q = 90$ W. The increase of φ is not very influential on the fully developed Nusselt number and it decreases monotonically along the tube length. This is because of the increase in the k value in the denominator of the Nusselt number relation. In other words, with increasing the φ value both the heat transfer coefficient and the heat conduction coefficient will increase but it has no significant effect on the Nusselt number.

The effect of nanoparticle volume concentration on the averaged heat transfer coefficient for various Reynolds

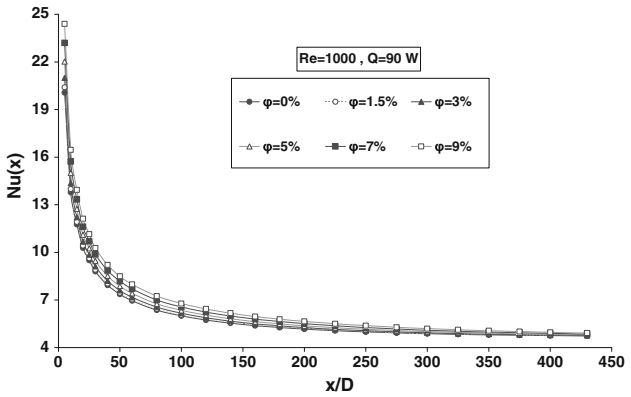

Fig. 7 The effect of solid volume fraction on the local Nusselt number of nanofluids for water as a base fluid

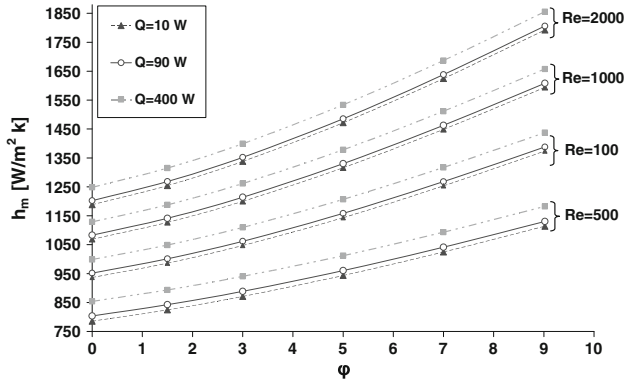

Fig. 8 The effect of solid volume fraction and power input on the averaged heat transfer coefficient for various Re No.

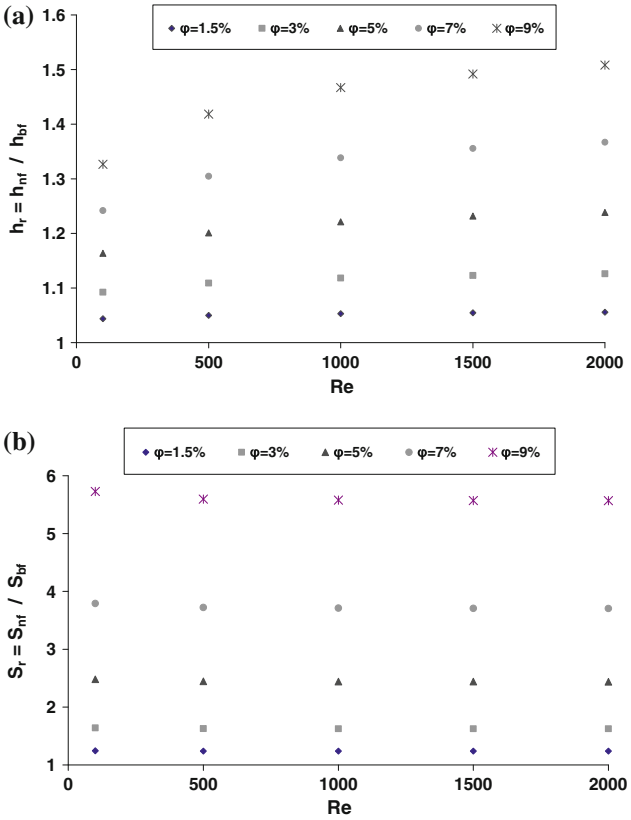

Fig. 9 The effect of solid volume fraction and Re No. for water-Al_2O_3 nanofluids at $Q = 10$ W. **a** Averaged heat transfer coefficient ratio. **b** Averaged shear stress ratio

numbers and heat transfer rate is shown in Fig. 8. It shows that in all of the Reynolds numbers the effect of heat transfer rate is the same. The maximum increase in h_m due to heat input (Q) is about 4% and has no significant effect. Figure 8 also depicts the enhancement of the averaged heat transfer coefficient by increasing Reynolds number or volume concentration of the nanoparicles. The maximum increase at each Reynolds number in $\varphi = 9\%$ is about 42% with respect to the base fluid.

The ratio of the averaged heat transfer coefficient in nanofluids (water-Al_2O_3) to the base fluid versus Reynolds number for various $\varphi \leq 9\%$ at $Q = 10$ W is shown in Fig. 9a. The figure presents that the averaged heat transfer coefficient ratio increases with increasing Re number and φ. At higher Reynolds numbers the increase is more in each φ and the maximum value of this ratio occurs for $\varphi = 9\%$ and is about 1.55. Figure 9b demonstrates the drastic undesirable effect of the wall shear stress in nanofluids. This figure depicts the ratio of the surface-averaged wall shear stress of nanofluid to base fluid over the entire length of the tube, versus Reynolds number. It is shown that this ratio increases violently by adding nanoparticles but it is approximately constant with variation of Reynolds number.

Figure 10a and b depict the ratio of the convective heat transfer coefficient and relative shear stress respectively, for nanofluid water-Al_2O_3 7% to the base fluid versus axial position at $Q = 400$ W. Figure 10a illustrates, with increasing the Reynolds number the non-dimensional h_r increases; however the enhancement gradually decreases along the tube length. Figure 10b displays the local shear stress ratio along axial direction for various Reynolds number. It is shown that in contrast with h_r, the local stress ratio decreases with increasing the Reynolds number, but this ratio; also increases along the tube length. It is contrary to the results for a particular φ, where local wall shear stress increases with increase in Re No. which will be described in the following.

The effect of Al_2O_3 nanoparticles volume concentration on the averaged wall shear stress for various Reynolds numbers and heat transfer rates in water base fluid is shown in Fig. 11. The averaged wall shear stress increases with increasing Reynolds number as well as φ and decreases with enhancing of the Q value. This is due to the reduction of the viscosity with increasing the temperature.

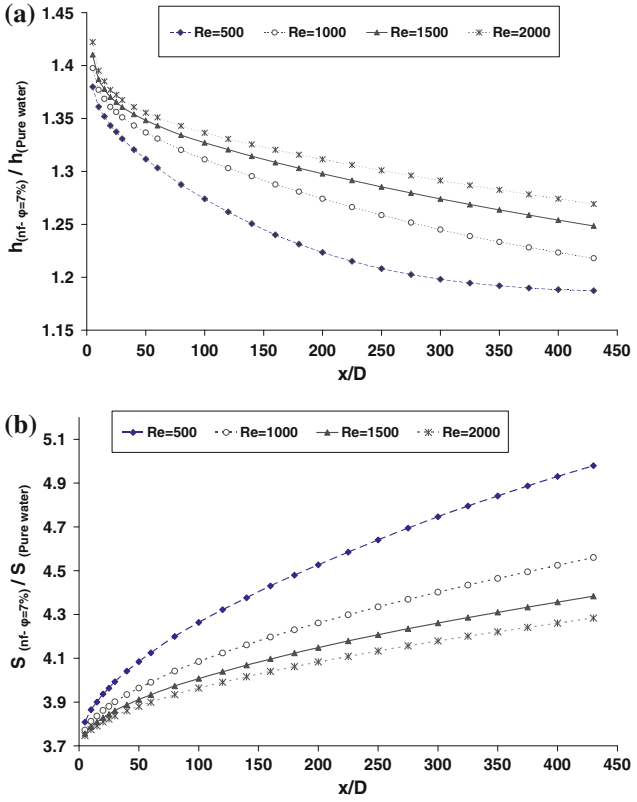

Fig. 10 The effect of Re No. for water-Al_2O_3 7% nanofluids at $Q = 400$ W. **a** Local heat transfer coefficient ratio. **b** Local wall shear stress ratio

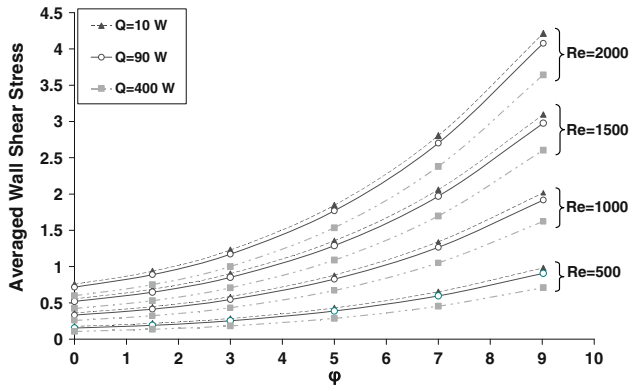

Fig. 11 The effect of solid volume fraction and heat input on the averaged wall shear stress for various Re No.

As shown in the Fig. 12a and b, the results show that the pressure drop and pumping power of the Al_2O_3-water increase with increasing Reynolds number and nanoparticle concentration. These figures show that the pressure drop and pumping power in the nanofluids at low solid volumetric concentration ($\varphi < 3\%$) is approximately the same as in the pure base fluid in the various Reynolds numbers, but the higher solid nanoparticle volume concentration causes a penalty drop in the pressure. However

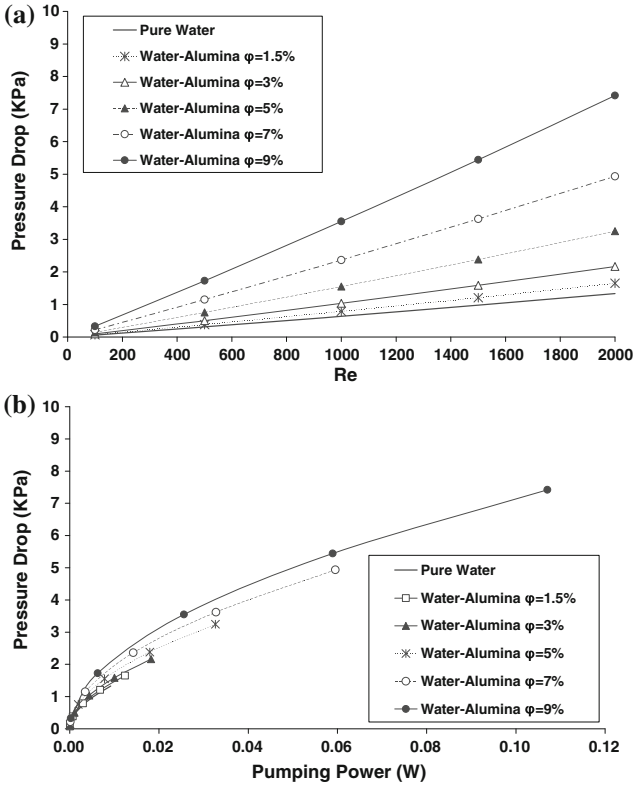

Fig. 12 The effect of Re No. for water-Alumina nanofluids at $Q = 10$ W. **a** Pressure drop. **b** Pumping power

this implies that the Al_2O_3—water nanofluid (specially $\varphi > 3\%$) incurs a need for additional pumping power, but the maximum power supply calculated for Al_2O_3 9% at Re = 2,000 is under 0.12 W and it is a hopeful sign for practical applications.

Figure 13 illustrates the influence of the 3% Al_2O_3 particles volume concentration on the wall and fluid mean bulk temperature versus local axial position at the Re = 1,000 and $Q = 10$ W in different base fluids. One can observe that the wall temperature and bulk fluid temperature decrease when the nanofluid is used instead of the base fluid and it seems to be more effective toward the exit plane. It is seen that the difference between wall temperature and bulk fluid temperature is minimum in EG-Al_2O_3 which means the convective heat transfer coefficient is increased more in this nanofluid with respect to the others. This is a desirable effect to decrease the wall temperature in the industrial usage, for example in heat exchangers.

The results of h_r at Re = 500, 1,000, and 2,000 are presented in Fig. 14 for water-Al_2O_3 and EG-Al_2O_3 with nanoparticle 3%. As it is shown in Fig. 14 the use of EG-Al_2O_3 has more benefit to increase heat transfer coefficient ratio with comparison to water-Al_2O_3. Noting the curves of Fig. 14 it can be seen that, the EG-Al_2O_3 nanofluid has the maximum jump in value of h_r with respect to the change of Reynolds number.

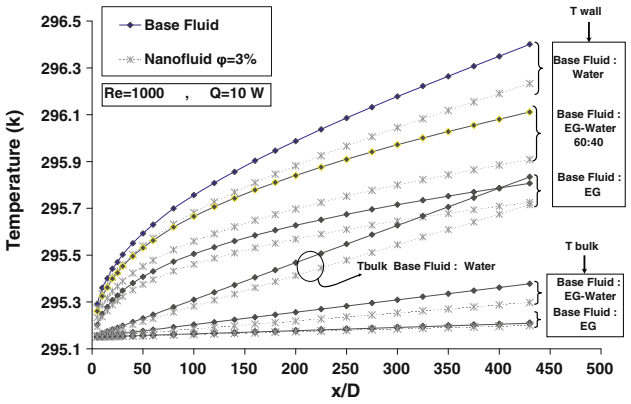

Fig. 13 The effect of different base fluids on the wall and fluid mean bulk temperature versus local axial position for $\varphi = 3\%$

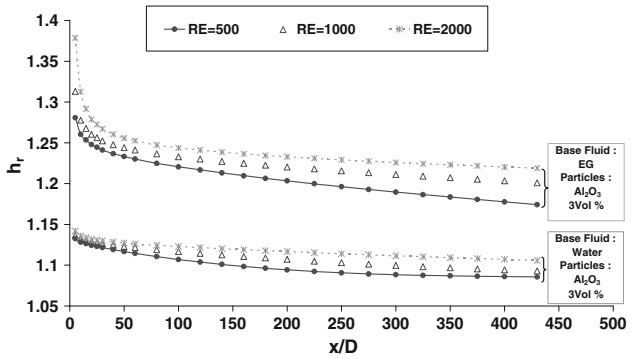

Fig. 14 The effect of different base fluids and Re No. on the local heat transfer coefficient ratio for $\varphi = 3\%$

Figure 15a, b show the averaged heat transfer coefficient and averaged wall shear stress for Re = 100 to 2,000 and different φ at $Q = 10$ W with considering two nanofluids, namely water-ethylene glycol mixture (60:40 by mass), and ethylene glycol with Al_2O_3 nanoprticles. The investigation of the comparison of different nanofluids in Fig. 15a and b can be an aid to achieve higher heat transfer coefficient with lower wall shear stress. The results indicate that the mean heat transfer coefficient and wall shear stress, increase with increasing of the three parameters, mass of ethylene glycol in the water base fluid, solid concentration, and Reynolds number. Figure 15a displays EG-Al_2O_3 3% has the greatest mean heat transfer coefficient at Reynolds number higher than or equal to 1,000, but in Re No. lower than 1,000 the maximum value occurs in EG-water-Al_2O_3 9%, and also it can be seen that in all ranges of the Reynolds number the mean heat transfer coefficient of EG-water-Al_2O_3 9% is more than pure EG. This is against the results obtained in Fig. 15b, where the first and second peak of averaged wall shear stress at each computed set of Re No. belong to EG-Al_2O_3 3%, and pure EG respectively. It is due to the effect of effective viscosity of the ethylene

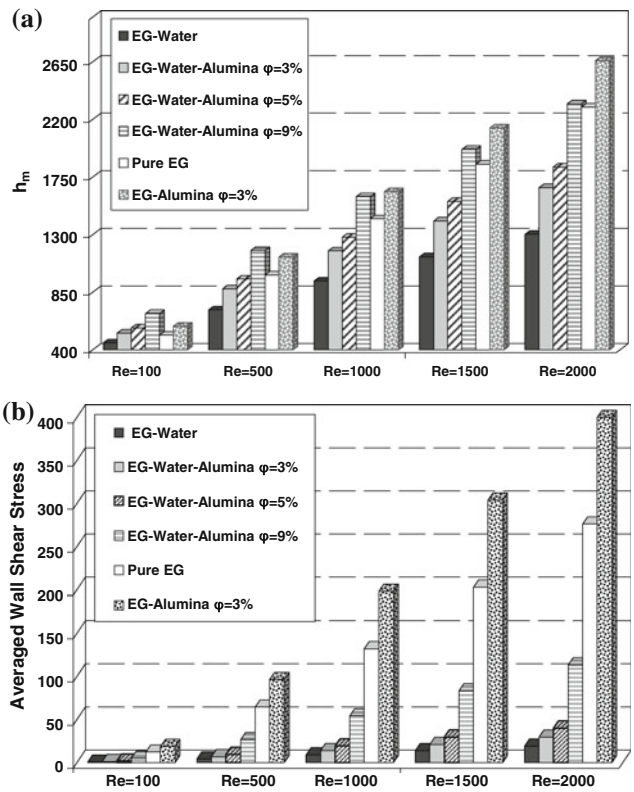

Fig. 15 The effect of solid volume fraction and different base fluid for various Re No. at $Q = 10$ W. **a** Averaged heat transfer coefficient **b** Averaged wall shear stress

glycol which is generally more than water and ethylene glycol water mixture (60:40) as shown in Table 1. Thus it is shown, from the present study on the water ethylene glycol mixture nanofluids, that it is practical to increase the mean heat transfer coefficient and decrease the wall shear stress with an augmentation of the volume fraction of nanoparticle to the ethylene glycol water instead of increasing the mass of ethylene glycol. At the other values of Q between the range of 10 to 400 W and with the other nanofluid, EG-water mixture (30:70), at all the computed concentration the same trend was observed.

5 Conclusion

The laminar convective flows of three stable nanofluids EG, water, and EG/water mixture and Al_2O_3 as nanoparticle in an axi-symmetric horizontal tube with different power inputs of $10 \leq Q \leq 400$, and varying Reynolds numbers of $100 \leq \mathrm{Re} \leq 2{,}000$ in a wide range of nanoparticle concentrations $0 \leq \varphi \leq 0.09$ are studied. All of the nanofluid properties in the present study depend on the temperature and nanoparticles volume concentration. The aim of this research is to investigate the comparison of

the different base fluid nanofluids to achieve a higher heat transfer rate with lower wall shear stress. The results indicate that the averaged heat transfer coefficient and wall shear stress increase with increasing three parameters, mass of ethylene glycol in the water base fluid, solid concentration and Reynolds number. It is seen, however, the ethylene glycol has a thermal conductivity lower than water, and the enhancement of k due to nanoparticle concentration of Al_2O_3 in EG is more than in water. The results show, the use of EG-Al_2O_3 has more benefit to enhance the heat transfer coefficient with comparison to water-Al_2O_3 and similarly with increasing the mass of EG in EG/water mixture the relative local heat transfer coefficient ratio (h_r) tends to increase along the axial positions. Also the results clearly show that by adding nanoparticles into the base fluid, the entrance region becomes to some extent larger which in turn causes the enhancement of convection heat transfer.

Thus the pressure drop and pumping power in the nanofluids at low solid volumetric concentration ($\varphi < 3\%$) is approximately the same as in the pure base fluid in the various Reynolds numbers, but the higher solid nanoparticle volume concentration causes a penalty drop in the pressure. Moreover it is shown, from the present study on the water ethylene glycol mixture nanofluids, that it is practical to increase the mean heat transfer coefficient and decrease the wall shear stress with an augmentation of the volume fraction of nanoparticle to the ethylene glycol water instead of increasing the mass of ethylene glycol.

References

1. Choi SUS (1995) Enhancing thermal conductivity of fluid with nanoparticles, developments and applications of non-newtonian flows, FED-vol. 231/MD 66:99–105
2. Eastman JA, Choi SUS, Li S, Thompson LJ, Lee S (1997) Enhancement thermal conductivity through the development of nanofluids. Procsymposium on nanophase and nanocomposite materials II, vol 457, Material research society, Boston, pp 3–11
3. Choi SUS, Zhang ZG, Yu W, Lockwood FE, Grulke EA (2001) Anomalously thermal conductivity enhancement in nanotube suspensions. Appl Phys Lett 79:2252–2254
4. Maxwell JC (1904) Treatise on electricity and magnetism. London, Cambridge, pp 435–441
5. Xuan Y, Li Q (2003) Investigation on convective heat transfer and flow features of nanofluids. J Heat Mass Transf 125:151–155
6. Choi S (1995) Enhancing thermal conductivity of fluid with nanoparticles. ASME Publ 66:99–105
7. Sohn CW, Chen MM (1981) Micro convective thermal conductivity in disperse two-phase mixtures as observed in a low velocity couette flow experiment. J Heat Mass Transf 103:45–51
8. Wen D, Ding Y (2004) Experimental investigation into convective heat transfer of nanofluid at the entrance region under laminar flow conditions. J Heat Mass Transf 47:5181–5188
9. Li Q, Xuan Y (2000) Experimental investigation of transport properties of nanofluids. In: Buxuan, Wang (ed) Heat transfer sci & technology, Higher Education Press, Beijing, pp 757–762
10. Wang XQ, Mujumdar AS (2007) Heat transfer characteristics of nanofluids: a review. Int J Thermal Sci 46:1–19
11. Roy G, Nguyen CT, Lajoie PR (2004) Numerical investigation of laminar flow and heat transfer in a radial flow cooling system with the use of nanofluids. Super lattices Microstruct 35:497–511
12. Maiga SEB, Palm SJ, Nguyen CT, Roy G, Galanis N (2005) Heat transfer enhancement by using nanofluids in forced convection flows. Int J Heat Mass Transf 26:530–546
13. Pak BC, Cho YI (1998) Hydrodynamic and heat transfer study of dispersed fluids with submicron metallic oxide particles. Exp Heat Transf 11:151–170
14. Palm SJ, Roy G, Nguyen CT (2006) Heat transfer enhancement with the use of nanofluids in radial flow cooling systems considering temperature dependent properties. Appl Thermal Eng 26:2209–2218
15. White FM (1991) Viscose fluid flow. McGraw Hill, New York
16. Xuan Y, Roetzel W (2000) Conceptions for heat transfer correlation of nanofluids. Int J Heat Mass Transf 43:3701–3707
17. Zhou SQ, Ni R (2008) Measurement of the specific heat capacity of water-based Al_2O_3 nanofluid. Appl Phys Lett 92:093123
18. Eastman JA, Choi SUS, Li S, Soyes G, Thormpson LJ, Di Melfi RJ (1999) Novel thermal properties of nanostructured materials. Material Sci Forum 312–314:629–634
19. Maiga SEB, Nguyen CT, Roy G, Galanis N (2004) Heat transfer behaviors of nanofluids in a uniformly heated tube. Super lattices Microstruct 35:543–557
20. Vajjha RS, Das DK (2009) Measurement of thermal conductivity of three nanofluids and development of new correlations. Int J Heat Mass Transf 52:4675–4682
21. Hamilton RL, Crosser OK (1962) Thermal conductivity of heterogeneous two-component systems. Ind Eng Chem Fundam 1:187–191
22. Zhang X, Gu H, Fujii M (2006) Effective thermal conductivity and thermal diffusivity of nanofluids containing spherical and cylindrical nanoparticles. Appl Phys 100(044325):1–5
23. Abu-Nada E (2009) Effect of variable viscosity and thermal conductivity of Al_2O_3-water nanofluid on heat transfer enhancement in natural convection. Int J Heat Fluid Flow 30:679–690
24. Nguyen CT, Desgranges F, Roy G, Galanis N, Mare T, Boucher S, Angue Minsta H (2007) Temperature and particle-size dependent viscosity data for eater-based nanofluids—hystersis phenomenon. Int J Heat Fluid Flow 28:1492–1506
25. Masuda H, Ebata S, Teramae K, Hishinuma N (1993) Alteration of thermal conductivity and viscosity of liquid by dispersing ultra-fine particles. In: Japanese, Netsu Bussei 4:227–233
26. Namburu PK, Das DK, Tanguturi KM, Vajjha RS (2009) Numerical study of turbulent flow and heat transfer characteristics of nanofluids considering variable properties. J Thermal Sci 48:290–302
27. ASHRAE Handbook (2005) Fundamentals, American Society of Heating, Refrigerating and Air-Conditioning Engineering Inc., Atlanta, GA
28. Patankar SV (1980) Numerical heat transfer and fluid flow. Hemisphere Publishing Corporation, New York
29. Ferziger JH, Peric M (1999) Computational method for fluid dynamics. Springer, New York
30. Kim D, Kwon Y, Cho Y, Li C, Choeong S, Hwang Y, Lee J, Hong D, Moon S (2009) Convection heat transfer characteristics of nanofluids under laminar and turbulent flow conditions. J Current Appl Phys 9:e119–e123
31. Shah RK, London L (1978) Laminar flow forced convection in ducts. Supplement 1 to advances in Heat transfer academic Press, New York

32. Keblinkski P, Phillpot SR, Choi SUS, Eastman JA (2002) Mechanisms of heat flow in suspensions of nano-sized particle (nanofluids). Int J Heat Mass Transf 45:855–863

33. Kakac S, Pramuanjaroenkij A (2009) Review of convective heat transfer enhancement with nanofluids. Int J Heat Mass Transf 52:3187–3196